# Analytical Modelling of Pulse Transformers for Power Modulators

J. Biela, D. Bortis, J. W. Kolar

Power Electronic Systems Laboratory (PES), ETH Zurich, Switzerland

E-Mail: biela@lem.ee.ethz.ch / Homepage: www.pes.ee.ethz.ch

*Abstract* – **The parasitic capacitances of transformers significantly influence the resulting pulse shape of a power modulator system. In order to predict the pulse shape and optimize the geometry of the pulse transformer before building the transformer an equivalent circuit and analytic expressions relating the geometry with the parasitic elements are needed. Therefore, a model consisting of 6 equivalent capacitors and a simplified circuit as well as the belonging equations are presented. The equations are verified by measurement results for a pulse transformer and a solid state modulator designed for linear accelerators.**

*Keywords*: Transformer model, parasitic capacitance, solid state modulator, analytic model

## I.  INTRODUCTION

High voltage and high power pulses are used in a wide variety of applications, for example in accelerators, radar, medical radiation production or ionization systems. In many of these applications the requirements on the generated pulses regarding for example rise/fall time, overshoot, pulse flatness and pulse energy are high. The pulses for these applications are usually generated with pulse modulators, which often use a pulse transformer for generating high output voltages. There, the parasitic elements of the transformer significantly influence the achievable shape of the pulse.

For predicting the pulse shape of the modulator system, for designing pulse forming networks and for optimizing the geometry of the pulse transformer before building the transformer an appropriate equivalent circuit of the transformer is needed. This equivalent circuit must on the one hand predict the transfer function of the transformer and on the other hand the parameters of the circuit should be analytically calculable with the geometric and electric parameters of the transformer. Therefore, an equivalent model of the pulse transformer and the analytic equations for calculating the parameters are presented in this paper.

In [1, 2] a simple L-L-C model of the transformer is used to predict the resulting pulse shape. The value of the capacitance in this model is calculated by applying the equation for parallel-plate capacitor [1] and for non parallel-plate capacitor [2] on the primary / secondary winding interface what results in

$$C_{\backslash/} = \frac{\varepsilon\, l_{Wdg} h_{Wdg}}{d_{Wdg}} \left( \frac{N-1}{N} \right)^2 \Bigg| C_{||} = \frac{\varepsilon\, l_{Wdg} h_{Wdg}}{d_{Wdg}} \left( \frac{N^2+N+1}{N^2} \right) \qquad (1)$$

In both, only the distributed electric energy in the volume between the primary and the secondary winding is considered, what results in a relatively poor accuracy. This could be seen in **figure 1** where a measured and two calculated pulse responses of a transformer are shown. The input voltage of the calculation models was the measured output voltage of the solid state switch.

In contrast to the prediction of the simple models the result of the extended model matches the measurement results much better. In this model all the regions which are relevant with respect to the distributed energy are considered.

Thus, in **section II** of the paper first the energies which are stored in the different relevant regions are calculated by analytic approxima-
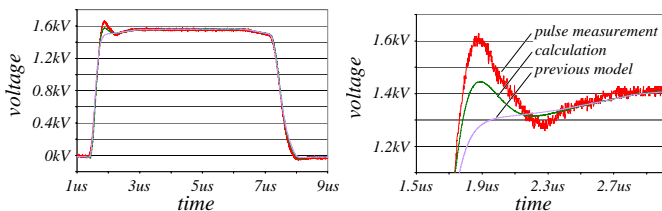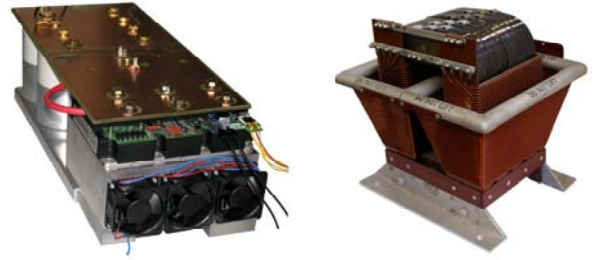


Figure 2. Solid state modulator (1kV/4kA) / transformer for measurement.

tions. In the next step the calculated energies are compared with the energies stored in the equivalent circuit in **section III**. By this comparison the parameters of the equivalent circuit of the pulse transformer are determined. The suggested model comprises six capacitors and could be used in any connection of the transformer. If both windings are grounded the model could be simplified to an equivalent circuit with just one capacitor. With the considerations of section II an equation is derived which allows the calculation of the equivalent capacitance by means of the transformer geometry. Based on this equation a good prediction of the pulse shape is possible as shown in figure 1.

Another possibility to obtain the parameter of the suggested equivalent circuit is to use 2D FEM-simulations. For this reason the setup of the simulations is explained in **section IV**. The described setups also could be used to parameterise the model by impedance measurements.

In **section V** the proposed equations are validated by comparing the calculated and the measured pulse shape for different operation and load conditions for a solid state pulse modulator. Finally, a conclusion is presented in **section VI**.

## II.  CALCULATION OF PARASITIC CAPACITANCES

For determining the equivalent capacitances of the pulse transformer's equivalent circuit the distributed energies in all regions must be calculated. In order to be able to calculate the stored energies the 3 dimensional distribution of the electric field strength must be known. The field distribution, however, generally only could be calculated with time consuming numeric FEM-simulations.

Since in most regions the run of the electric flux lines approximately lies within a plane which is parallel to the winding axis, the per unit energies for these planes are considered in the following. In **figure 3** a 2D cut of the transformer with surrounding tank is given. There, six different planes/regions are shown which are considered in the following for calculating the stored energy.

Since the calculations are performed for planes per unit energies result. In order to obtain the value of the stored energy of the respective region the per unit energy must be
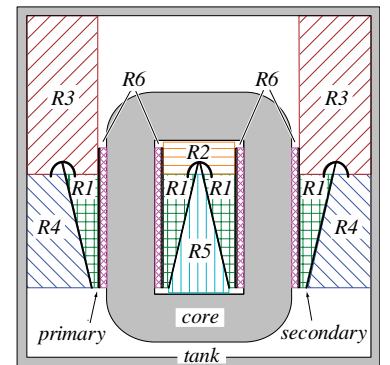


Figure 1. Comparison of measurement and the two different calculations



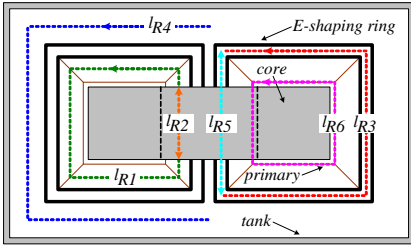Figure 3.  Regions for the distributed capacitance of the pulse transformer.

Figure 4. Definition of the lengths for the distributed capacitances.

culations are performed for a pulse transformer with non parallel-plate windings. However, the presented procedure can analogically applied to other winding arrangements, e.g. transformer with parallel windings. Furthermore, it is assumed that the core and also the tank is grounded what is usually true in practice.

In the following paragraphs the stored energies for the six regions are calculated separately. There, the presented equations always represent the part of the energy which is stored in the winding of one leg, that means that for example the energies must be multiplied by two for the setup shown in figure 3.

### A. Energy between the windings – R1

In region $R_1$ the area between the primary and the secondary winding is summarised. This is the only area which is considered for determining the equivalent circuit of the pulse transformer in the approach presented in [1, 2] – cf. equation (1).
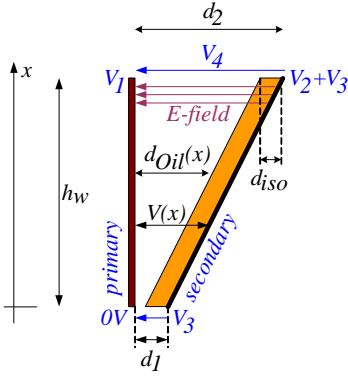


Figure 5. Calculation of the energy $W_{R1}$ by means of the parallel plate capacitor

For simplifying the calculation of the energy $W_{R1}$ between the primary and the secondary it is assumed in the following that both windings consist of a conductive plate with a linear voltage distribution. The primary winding is grounded at the lower side and the voltage at the upper end is $V_1$, whereas the voltage distribution of the secondary winding starts at the offset voltage $V_3$ and ends at $V_2+V_3$ as shown in figure 5. In case the secondary winding is also grounded voltage $V_3$ is zero.

With the assumed voltage distribution the voltage difference between the two plates and the distance between the two plates could be written as

$$V(x) = \frac{x}{h_w}(V_4 - V_3) + V_3 \quad \bigg| \quad d(x) = d_{Oil}(x) + d_{Iso} = \frac{d_2 - d_1}{h_w} x + d_1 \quad (2)$$

There, $d_1$ is the distance at the lower end and $d_2$ at the upper end.

In order to simplify the calculations further, the electric flux lines between the primary and the secondary winding in region $R_1$ are approximated by straight lines which are orthogonal to the primary winding. In this case the energy stored in the differential element $dx$ could be calculated by

$$dW'_{R1} = \frac{\varepsilon V^2(x)}{2(d_{Oil}(x) + d_{Iso})} dx = \frac{\varepsilon}{2} \frac{\left((V_4 - V_3)x + V_3 h_W\right)^2}{\left((d_2 - d_1)x + d_1 h_W\right)h_W} dx \quad (3)$$

Integrating this expression along the primary winding yields the total per unit energy $W'_{R1}$ which is stored in the plane $(R_1)$ between the two plates. Multiplying the per unit energy by the length $l_{R1}$ (cf. fig. 4) yields the energy $W_{R1}$ stored in region $R_1$.

multiplied by the lengths shown in **figure 4**.

The areas/volumes which are not covered by a region are neglected in the following, since the energy density and therewith the share in the total equivalent capacitance is relatively small.

The presented cal-

$$W_{R1} = l_{R1} \int_0^{h_w} \frac{\varepsilon}{2} \frac{\left((V_4 - V_3)x + V_3 h_W\right)^2}{\left((d_2 - d_1)x + d_1 h_W\right)h_W} dx \quad (4)$$

In general, this energy depends on the voltage difference between the two plates and also on the offset voltage of the secondary winding.

So far it has been assumed that the materials between the two plates have the same permittivity $\varepsilon_{Iso}= \varepsilon_{Oil}=\varepsilon$. Usually, the space between the two windings is filled with oil and the coil former of the secondary winding. If these two materials have a different permittivity an equivalent value for the permittivity could be calculated by

$$\varepsilon_{eq}(x) = \frac{\varepsilon_{Iso} \cdot \varepsilon_{Oil} \cdot (d_{Iso} + d_{Oil}(x))}{\varepsilon_{Iso} \cdot d_{Oil}(x) + \varepsilon_{Oil} \cdot d_{Iso}} . \quad (5)$$

This equivalent permittivity is a function of $x$ since the path length of the field line in the oil varies with $x$. Substituting the permittivity in equation (3) by this expression and calculating the energy results in

$$W_{R1} = \int_0^{h_w} \frac{l_{R1} \varepsilon_{Iso} \varepsilon_{Oil} \left((V_4 - V_3)x + V_3 h_W\right)^2 2^{-1} dx}{\left(\varepsilon_{Iso}\left[(d_2 - d_1)x + (d_1 - d_{Iso})h_W\right] + \varepsilon_{Oil} d_{Iso}h_W\right)h_W} . \quad (6)$$

Again, the voltage $V_3$ could be set to zero if the secondary windings is also grounded and the voltage $V_4$ could be substituted by $V_4 = V_2 - V_1$.

### B. Winding window: above secondary – R2

Region $R_2$ consists of the area above the secondary winding within the winding window. The border of this region has a complex shape which is determined by the core, the primary winding and the E-field shaping ring. In order to be able to calculate the distributed capacitance of this region analytically the geometry is simplified as shown on **figure 6**. First, it is assumed that the primary winding consists of a metal plate which is grounded, i.e. $V_1$ is neglected since $V_2 = N \cdot V_1 \gg V_1$. Furthermore, this plate is extended so that the upper end touches the core. Second, the secondary winding is neglected and the E-field shaping ring is replaced by a circle. This simplifications result in a coaxial structure which energy is approximately ($\pm 10\%$) the same as the one of the original structure as could be proven by FEM-simulations.

The energy stored in the coaxial structure in **figure 7(a)** could be calculated with the equation for the cylindrical capacitor, what results in the per unit equation

$$W'_{R2} = \frac{1}{4} \frac{\pi \varepsilon_{Oil}}{\ln(r_o/r_i)}(V_2 + V_3)^2 = \frac{\pi \varepsilon_{Oil}(V_2 + V_3)^2}{4\ln(k\, d/r_i)} \quad \text{with} \quad k = 1.08. \quad (7)$$

There, only one half of the energy is calculated since the equations represent the part of the energy which is stored in the winding of one leg. i.e. half the region $R_2$.

The factor $k$ is empirically determined by FEM-simulations so that the resulting difference between the energy of the original structure and the equivalent one is minimal. In [3] a similar transformation is described but the factor k is set equal to 1.16. For the considered setup, this choice resulted in a larger error for the equivalent energy than k=1.08.

In order to obtain the energy $W_{R2}$ the per unit energy $W'_{R2}$ must be multiplied by $l_{R2}$.

### C. Above secondary winding outside winding window – R3

Region $R_3$ is the equivalent of region $R_2$ outside the winding window, but there the run of the border in the upper region is more complex.
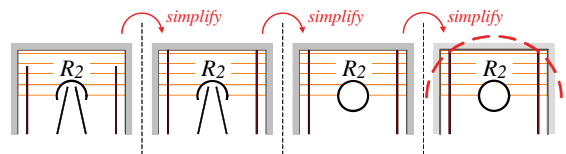


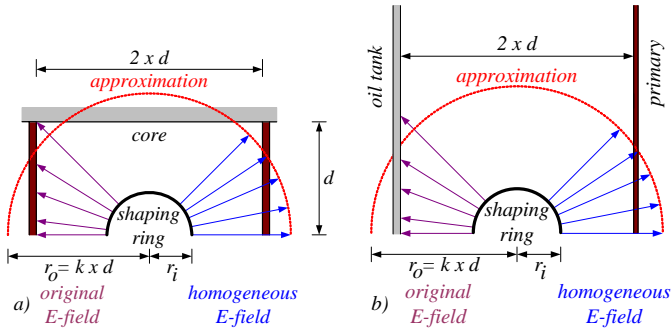Figure 6. Simplification of the region $R_2$ to a coaxial structure.

Figure 7. (a) Equivalent structure for calculating the energy of region $R_2$. (b) Original and simplified geometry for region $R_3$.

For simplifying the setup it is assumed that the primary winding consists of a grounded plate (i.e. neglect $V_1 << V_2$) which is stretched to the cover of the tank. The influence of the cover itself is neglected since its distance to the E-field shaping ring is relatively large (cf. fig. 3). Furthermore, it is assumed that the E-field shaping ring is in the middle of the primary winding and the wall of the tank, what is approximately fulfilled for a compact design, where the distance between the E-field shaping ring and the tank is equal to the minimum possible one.

The resulting rectangular border is again approximated by a coaxial structure as shown in **figure 7(b)**. With this approximation the stored energy for this structure could be calculated by

$$W_{R3} = \frac{l_{R3}}{2} \frac{\pi \varepsilon_{Oil}}{\ln(k\,d/r_i)} (V_2 + V_3)^2 \text{ with } k = 1.275, \quad (8)$$

where $k$ is empirically adapted by FEM-simulations again. For this structure the value which results in a minimum error is 1.275, which is the same as proposed in [2].

*Remark*: In case the transformer is not inside a grounded tank the plate on the left hand side in figure 7(b) is be omitted. There, the geometry could be simplified by assuming that the primary winding is grounded and extended to infinity so that the energy in this region could be calculated with the equations for the capacitance of two wire lines. This results in

$$W_{R3,II} = l_{R3} \frac{\pi \varepsilon_{Oil}}{\ln\left(2d/r_i - + \sqrt{(2d/r_i)^2 - 1}\right)} \quad (9)$$

for the energy stored in region $R_3$.

### D.    Between secondary and tank – R4

The energy between the secondary and the wall of the tank below the E-field shaping ring is partially included in region $R_4$. There, the wall of the tank and the secondary winding form a non-parallel plate capacitor with a approximately linear voltage distribution again. The voltage and the distance between the plates are given as a function of $x$ by

$$V(x) = \frac{x}{h_w} V_2 + V_3 \quad \Big| \quad d(x) = \frac{d_2' - d_1'}{h_w} x + d_1', . \quad (10)$$

where the variables are defined as shown in **figure 8(a)**. Using these expressions the energy could be calculated by

$$W_{R4} = l_{R4} \int_0^{h_w} \frac{\varepsilon_{Oil}}{2} \frac{(V_2 x + V_3 h_w)^2}{((d_2' - d_1')x + d_1' h_w) h_w} dx \quad (11)$$

as described in section II.A.

Assuming a compact system, the distances could be set to $d'_2 = d_2$ and $d'_1 = 2d_2 - d_1$ as also has been done for region $R_3$.

In figure 8(b) a plot of the simulated electric flux lines between the secondary winding and the tank is shown. There, it could be seen that especially at the upper and the lower end of the winding (blue

circles) the run of the simulated flux lines deviates from the one which has been assumed in the calculation model for region $R_4$. At the upper end the reason for the deviation is the E-field shaping ring. At the lower end the field is mainly distorted by the voltage distribution on the secondary an



Figure 8. (a) Definition of the variables for region $R_4$. (b) Electric flux lines between the secondary winding and the wall of the tank.

also by the proximity of the core and the primary winding.

These deviations result in a reduced accuracy of the explained calculation method for region $R_4$. The exact run of the flux lines, however, just could be calculated with time consuming FEM-simulations. Furthermore, due to the small share of the energy stored in these parts of region $R_4$ in the overall stored energy the resulting overall error for calculating the effective capacitance is acceptable.

*Remark*: In case the transformer is not inside a grounded tank the deviations at the lower end of the secondary winding shown in the blue circle in figure 8(b) increase. That means that the electric flux lines at the left side of the secondary winding in figure 8(b) tend to start at the upper end of the winding and end at the lower end. Unfortunately, the energy stored within this field distribution could not be easily calculated with the approaches used here. Instead of that the energy is calculated by FEM-simulations.

### E.    Winding window: below secondary – R5

In the next step the energy stored in region $R_5$, i.e. below the secondary winding in the winding window, is calculated. There, the electric flux lines are approximated by straight lines again. These lines start at the secondary winding and are orthogonal to the winding window of the grounded core as shown in **figure 9(a)**.

With this approximation the stored energy could be calculated as described in section II.A for region $R_1$. The resulting equations are

$$V(x) = \frac{x}{d_2 - d_1} V_2 + V_3 \quad \Big| \quad d(x) = \frac{h_w}{d_2 - d_1} x + d_0 . \quad (12)$$

and

$$W_{R5} = l_{R5} \int_0^{d_2 - d_1} \frac{\varepsilon_{Oil} \left((d_2 - d_1)V_3 + V_2 x\right)^2}{2(d_2 - d_1)(d_0(d_2 - d_1) + h_w x)} dx , \quad (13)$$

where the evaluated integral is given in the appendix again.

Due to the limited volume and the low average energy density the stored energy usually is relatively small and could be neglected in
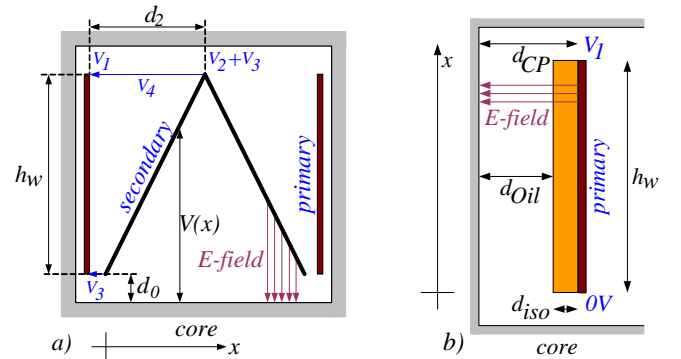


Figure 9. (a) Variables / simplified run of electric flux lines for region $R_5$. (b) Definition of variables for region $R_6$

many cases.

## F. Area between primary and core - $R_6$:

Finally, the energy stored between the primary winding and the core is calculated. This structure acts like a parallel plate capacitor with two different dielectrics – the oil and the coil former of the primary winding as shown in **figure 9(b)**. Assuming a linear voltage distribution again, the voltage distribution, the distance and the permittivity are

$$V(x) = \frac{x}{h_W}V_1 \quad \bigg| \quad d(x) = d_{Oil,P} + d_{Iso,P}$$

$$\varepsilon_{eq} = \frac{\varepsilon_{Iso}\varepsilon_{Oil}(d_{Iso,P} + d_{Oil,P})}{\varepsilon_{Iso}d_{Oil,P} + \varepsilon_{Oil}d_{Iso,P}} \tag{14}$$

and the energy could be calculated by

$$W_{R6} = l_{R6}\frac{1}{6}\frac{\varepsilon_{Iso}\varepsilon_{Oil}(d_{Iso,P} + d_{Oil,P})h_W}{(\varepsilon_{Iso}d_{Oil,P} + \varepsilon_{Oil}d_{Iso,P})d_{CP}}V_1^2. \tag{15}$$

## G. Winding capacitance

So far, only the stored energy/capacitances between the windings or between one winding and the core/tank have been considered. But also between the singe turns of one winding electric energy is stored. This energy could be calculated by approaches presented in [5-7].

Due to fact that the windings are usually implemented with only one or two layers and the turn to turn voltage is relatively small as well as the distance between the single turns is relatively large this part of the stored energy could be neglected.

## III. EQUIVALENT CIRCUIT OF PULSE TRANSFORMER

In the last preceding section the energies stored in the different regions of the pulse transformer/tank setup have been calculated. In the next step the parameters of the equivalent circuit of this setup are calculated. This is performed by comparing the energy stored in the equivalent circuit, which is a function of $V_1$-$V_3$, with the calculated stored energy, which is also a function of $V_1$-$V_3$. For determining the energy stored in the equivalent circuit, first an appropriate equivalent circuit must be chosen.

As could be shown the electrostatic behaviour of an arbitrary transformer could be modelled by a three input multipole (primary and secondary voltage and the voltage between the windings) [3]. In the linear working area and as long as propagation times can be ignored, the electrostatic energy / behaviour of this multipole could be modelled by six independent capacitors as shown in **figure 10**.

The energy stored in the equivalent circuit is given by

$$W_{Eq} = \frac{1}{2}\left(\begin{matrix} C_1V_1^2 + C_2V_2^2 + C_3V_3^2 + C_4(V_2 + V_3 - V_1)^2 \\ + C_5(V_2 + V_3)^2 + C_6(V_1 - V_3)^2 \end{matrix}\right), \tag{16}$$

what results from $1/2\,CV_C^2$. In the same manner the calculated energy could be written

$$W_{Cal} = 2(W_{R1} + W_{R2} + W_{R3} + W_{R4} + W_{R5} + W_{R6})$$
$$= f(V_1, V_2, V_3), \tag{17}$$

where $V_4$ has been replaced by $V_4 = V_2 + V_3 - V_1$ and the factor 2 results from the fact that the energies have been calculated for each leg separately.

Since both energies must be equal $W_{Eq} = W_{Cal}$ the equations of the capacitors can be derived by
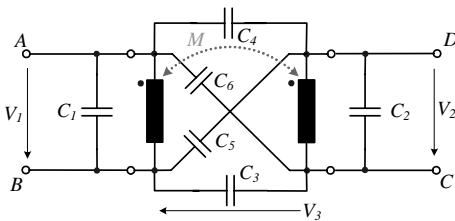


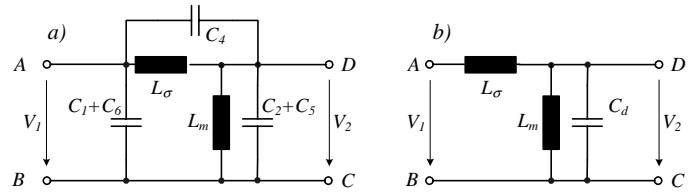Figure 10. General equivalent circuit of pulse transformer.



Figure 11. (a) Simplified equivalent circuit (cf. fig.10). (b) Approximated simplified circuit with capacitances transferred to secondary side.

setting the coefficients of the variables/voltage terms $V_1$, $V_2$, $V_3$, $V_1V_2$, $V_1V_3$ and $V_2V_3$ equal. This results in six independent equations which can be solved for the capacitances $C_1$-$C_6$.

In contrast to the results published in [3] the capacitors $C_1/C_2$, $C_3/C_4$ and $C_5/C_6$ are not interdependent since the windings are not arranged in parallel and therefore the winding construction is not symmetric with respect to the low and the high side.

With the described model the transfer behaviour of the pulse transformer and therewith the influence on the transferred pulse shape could be calculated and/or simulated for arbitrary connections. Moreover, with the equations relating the geometry of the transformer directly with the capacitances of the equivalent model the construction of the transformer could be optimized for the required transfer behaviour.

## A. Simplified circuit with new equations

In many pulse power applications the pulse transformer is not used for galvanic isolation and the low side of the primary as well as the low side of the secondary winding are grounded, i.e. $V_3 = 0$ in figure 10. In this case capacitor $C_3$ is replaced by a short circuit and $C_1/C_6$ as well as $C_2/C_5$ are in parallel. Moreover, the voltages across all capacitors could be derived from the primary and/or secondary voltage by using the turns ratio $N$. With the voltages known the energy which is stored in the capacitors could be calculated as a function of the secondary (or primary) voltage.

$$W = \frac{C_1 + C_6 + C_4(N-1)^2 + (C_2 + C_5)N^2}{2}V_2^2 = \frac{C_d}{2}V_2^2 \tag{18}$$

Furthermore, the equivalent circuit could be simplified to the circuit shown in **figure 11(a)**. Neglecting the parallel resonance between the leakage and capacitor $C_4$ this circuit could be further simplified to the circuit shown in figure 11(b), where only one capacitor is used which is transferred to the secondary side.

The capacitance value for the equivalent capacitor referred to the secondary side is

$$C_d = \frac{C_1 + C_6}{N^2} + \frac{C_4(N-1)^2}{N^2} + (C_2 + C_5) \tag{19}$$
$$\Rightarrow C_d \sim C_2 + C_4 + C_5 \text{ for large } N$$

The circuit of figure 13(b) is the same as used in [1, 2] but in those publications no equation for calculating the equivalent capacitance $C_d$ from the geometry of the transformer was given except for the simple parallel plate approach for the region between the windings.

## IV. DETERMINATION OF THE EQUIVALENT CIRCUIT BY FEM-SIMULATION OR MEASUREMENT

Besides the presented possibility to calculate the values of the six capacitors of the general equivalent circuit (cf. fig. 10) by means of the transformer geometry it is also possible to obtain the values by measurement or by FEM-simulation.

Since there are six independent capacitors in the equivalent circuit, six independent simulations / measurements must be carried out. The belonging measurement setups are shown in **figure 12**.

For the measurement results following below the values of the capacitances have been determined by using resonance peaks in the
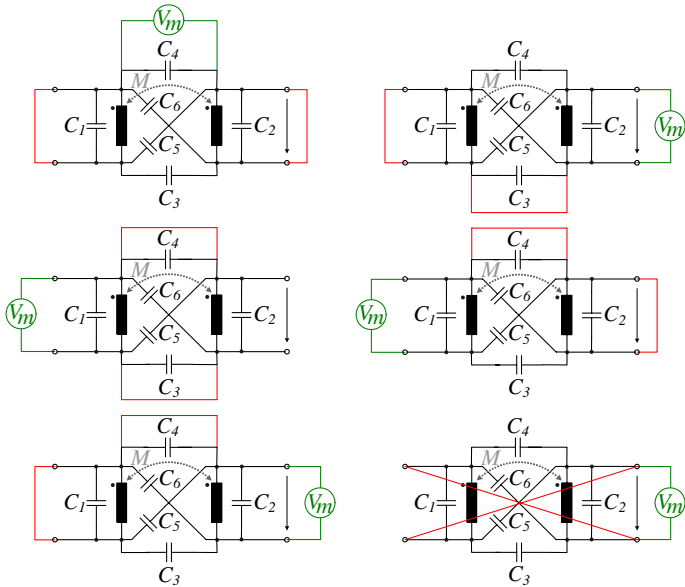
Figure 12. Measurement for determining the equivalent capacitances.

impedance plot. The required inductance values are directly measured with the impedance analyzer Agilent 4294A and then the capacitances are calculated with the frequency of the resonance peak.

With the measured capacitances the values of the equivalent capacitors of the circuit in figure 10 could be calculated by the following equations.

$$C_1 = \frac{1}{2}(C_{M2} - C_{M3} - C_{M4} + C_{M6}) \quad C_2 = \frac{1}{2}(-C_{M1} + C_{M3} + C_{M4})$$
$$C_3 = \frac{1}{2}(-C_{M2} + C_{M3} + C_{M5}) \qquad C_4 = \frac{1}{2}(C_{M1} - C_{M3} - C_{M5} + C_{M6}) \quad (20)$$
$$C_5 = \frac{1}{2}(C_{M4} + C_{M5} - C_{M6}) \qquad C_6 = \frac{1}{2}(C_{M1} + C_{M2} - C_{M4} - C_{M5})$$

Instead of measuring the capacitances with an impedance analyzer, the same setups could be used for determining the capacitances by FEM-simulations. There, either 3D simulations, which are quite accurate but very time consuming, or 2D simulations, which are much faster but less accurate, could be performed. The equivalent capacitors could be calculated with the same equations (20) as used for the measurements.

In **table 1** measurement, simulation and calculation results for a transformer are given. There, it could be seen that the values correspond very well.

**Table 1 -** Values for $C_{M1}$ - $C_{M6}$ for measurements, simulation and analytic calculation for the transformer in air without tank.

| No. | Measured | Simulated | Calculated |
|-----|----------|-----------|------------|
| 1 | 418 pF | 446 pF | 428 pF |
| 2 | 121 pF | 138 pF | 127 pF |
| 3 | 335 pF | 394 pF | 393 pF |
| 4 | 58 pF | 53pF | 49 pF |
| 5 | 190 pF | 167 pF | 141 pF |
| 6 | 150 pF | 133 pF | 153 pF |

## V. MEASUREMENT RESULTS

In order to verify the presented equations measurements at the pulse transformer shown in figure 2 excited by the solid state modulator also shown in figure 2 have been carried out. The measurements have been conducted at relatively low voltage (<2kV) so that very fast and accurate probes could be used and measurement errors related to voltage dividers could be avoided. Furthermore, during the measurements both windings were grounded, i.e. $V_3 = 0$, and the transformer was not inside a tank since none was available at the time of measurement. Further measurement results with tank and also loss equations will be presented in a future paper.

The equivalent circuit calculated for the transformer shown in figure 2 is given in **figure 13**. There, also the leakage inductance and the magnetising inductance are shown, which can be calculated from the magnetic field distribution in the window / core.



Figure 13. Calculated equivalent circuit for the transformer in figure 2.

In **figure 14** measured pulse responses are shown. Additionally, curves resulting from the model with six capacitors where the capacitance values have been determined by analytic calculations, simulations and impedance measurements are shown. There, it could be seen that the pulse shape including ringing could be predicted very well by means of the presented set of new equations.
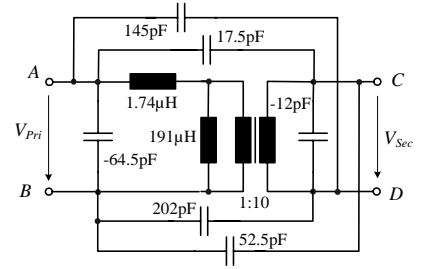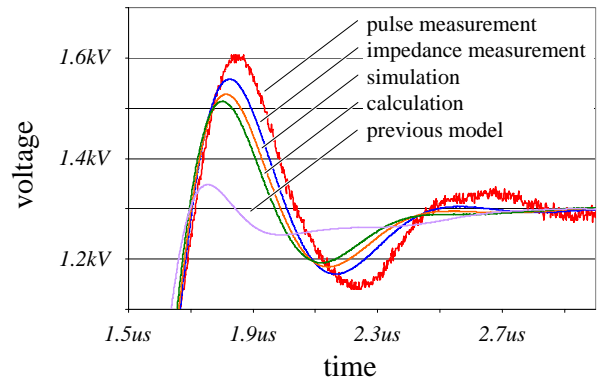


Figure 14. Measured, simulated and calculated pulse for 1500Ohm load.

## VI. CONCLUSION

In this paper a general model for pulse transformer which allows for predicting the pulse shape of a modulator system before building the transformer is presented. The parameters of the model can be analytically calculated from the geometry of the transformer or can be determined by simulation or measurement.

If both windings are connected to ground the presented model could be simplified to the known L-L-C. Furthermore, from the equations of the general model, analytic expressions for determining the parameters of the simple model based on the energy distribution in all relevant regions of the transformer are derived.

Both, the general and the simplified model based on the new equations show a good correspondence with the presented measurement results.

## REFERENCES

[1] N. G. Glasoe and J. V. Lebacqz, "Pulse Generators", MIT Radiation Laboratory Series, vol. 5, McGraw-Hill Book Company, New York, 1948
[2] M. Akemoto, S. Gold, A. Krasnykh and R. Koontz, "Pulse Transformer R&D for NLC Klystron Pulse Modulator", SLAC, Stanford University
[3] Harold A. Wheeler, "Transmission-Line Properties of a Round Wire in a Polygon Shield".
[4] B. Cogitore, J.-P. Keradec, J. Barbaroux, "The two-winding transformer: an experimental method to obtain a wide frequency range equivalent circuit", Trans-action on Instrumentation and Measurement, Vol. 43, April, 1994, pp. 364 – 371.
[5] A. Massarini, M.K. Kazimierczuk, "Modelling the Parasitic Capacitance of Inductors", 16 Capacitor and Resistor Technology Symposium 96, 1996, March 11-15, pp. 78–85.
[6] A. Massarini, M.K. Kazimierczuk, G.Gandi, "Lumped Parameter Models for Single- and Multiple-Layers Inductors ", 27th Power Electronics Specialists Conference PESC '96, Vol. 1, June 23-27, 1996, pp. 295 – 301.
[7] J. Biela and J.W.Kolar, "Using Transformer Parasitics for Resonant Converters – A Review of the Calculation of the Stray Capacitance of Transformers", Conference Record of the IEEE Industry Applications Conference, Hong Kong, Oct. 2-6, 2005.